European Journal of Nutrition (2022) 61:85–99
https://doi.org/10.1007/s00394-021-02627-8

ORIGINAL CONTRIBUTION

Lactobacillus coryniformis MXJ32 administration ameliorates azoxymethane/dextran sulfate sodium-induced colitis-associated colorectal cancer via reshaping intestinal microenvironment and alleviating inflammatory response

Tao Wang[1] · Leshan Zhang[1] · Panpan Wang[1] · Yilin Liu[1] · Gangtu Wang[1] · Yuanyuan Shan[1] · Yanglei Yi[1] · Yuan Zhou[1] · Bianfang Liu[1] · Xin Wang[1] · Xin Lü[1]

Received: 2 March 2021 / Accepted: 24 June 2021 / Published online: 29 June 2021
© Springer-Verlag GmbH Germany, part of Springer Nature 2021

Abstract

Purpose Gut microbiota has been reported to contribute to either prevent or promote colorectal cancer (CRC), and treatment with probiotics might be a promising intervention method. The present study aimed to evaluate the potential anti-CRC effects of *Lactobacillus coryniformis* MXJ32 on a colitis-associated (CA)-CRC mouse model.

Methods The CA-CRC mouse model was induced by a single intraperitoneal injection of 10 mg/kg azoxymethane and followed by three 7-day cycles of 2% dextran sulfate sodium in drinking water with a 14-day recovery period. Mice were supplemented with *L. coryniformis* MXJ32 by oral gavage (1×10^9 CFU/day/mouse). The CA-CRC attenuating effects of this probiotic were assessed via intestinal barrier integrity, inflammation, and gut microenvironment.

Results Treatment with *L. coryniformis* MXJ32 could significantly inhibit the total number of tumors and the average tumor diameter. This probiotic administration prevented the damage of intestinal barrier function by enhancing the expression of tight junction proteins (Occludin, Claudin-1, and ZO-1) and recovering the loss of goblet cells. Moreover, *L. coryniformis* MXJ32 alleviated intestinal inflammation via down-regulating the expression of inflammatory cytokines (TNF-α, IL-1β, IL-6, IL-γ, and IL-17a) and chemokines (Cxcl1, Cxcl2, Cxcl3, Cxcl5, and Ccl7). In addition, *L. coryniformis* MXJ32 supplementation increased the abundance of some beneficial bacteria (such as SCFAs-producing bacteria, *Lactobacillus*, *Bifidobacterium*, *Akkermansia*, and *Faecalibaculum*) and decreased the abundance of some harmful bacteria (such as pro-inflammatory bacteria, *Desulfovibrio* and *Helicobacter*), which in turn attenuated the overexpression of inflammation.

Conclusion *Lactobacillus coryniformis* MXJ32 could effectively ameliorate CA-CRC via regulating intestinal microenvironment, alleviating inflammation, and intestinal barrier damage, which further suggested that *L. coryniformis* MXJ32 could be considered as a functional food ingredient for the alleviation of CA-CRC.

✉ Bianfang Liu
bfliu9509@163.com

✉ Xin Wang
wangxin_2018@nwsuaf.edu.cn

✉ Xin Lü
xinlu@nwsuaf.edu.cn

[1] College of Food Science and Engineering, Northwest Agriculture and Forestry University, No. 22 Xinong Road, Yangling District, Xianyang 712100, Shaanxi, China

Graphic abstract

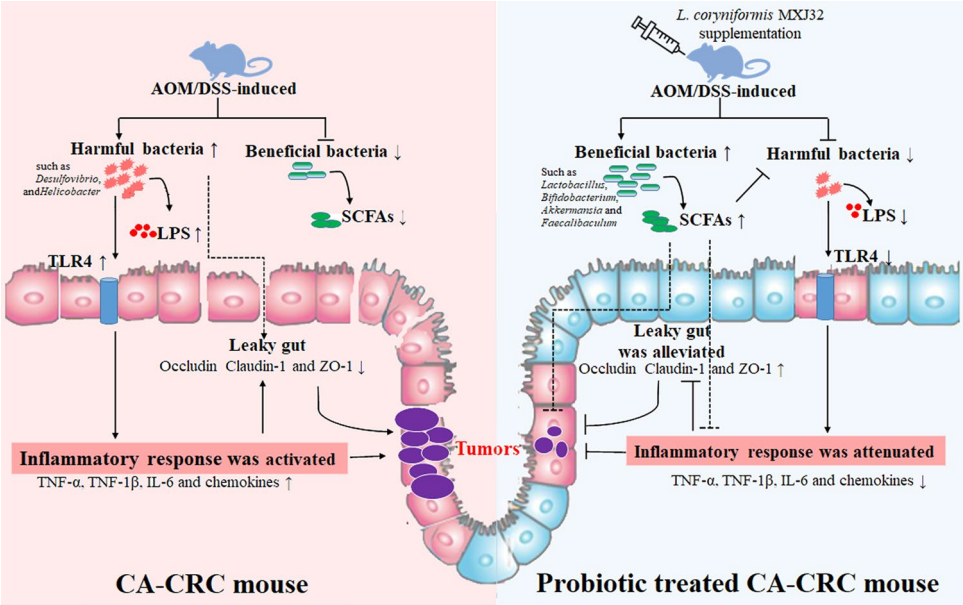

Keywords *Lactobacillus coryniformis* · Colorectal cancer · Gut microbiota · Inflammation · Intestinal permeability

Abbreviations

ANOVA	Analysis of variance
AOM	Azoxymethane
CA-CRC	Colitis-associated colorectal cancer
CFU	Colony forming unit
CXCR	C-X-C motif receptor
DAI	Disease activity index
DSS	Dextran sulfate sodium
FITC	Fluorescein isothiocyanate
H&E	Hematoxylin and eosin
IL	Interleukin
LDA	Linear discriminant analysis
LEfSe	Linear discriminant analysis effect size
LPS	Lipopolysaccharides
MUC	Mucin
OUT	Operational taxonomic unit
PCoA	Principal coordinates analysis
SCFA	Short-chain fatty acid
TFF	Trefoil factor
TLR	Toll-like receptor
TNF	Tumor necrosis factor
TUNEL	Terminal deoxynucleotidyl transferase dUTP nick end labeling
UPGMA	Unweighted pair group method with arithmetic mean
ZO-1	Tight junction protein-1

Introduction

Colorectal cancer (CRC), one of the most common cancers, ranked third in incidence and second in mortality [1]. Although several therapeutic options, including chemotherapy, radiation therapy, and immunotherapy are available, these methods may lead to serious adverse effects and the prognosis of CRC patients remains poor [2, 3]. Therefore, some new safe and effective preventive and/or therapeutic strategies are urgently needed for CRC.

Although the pathogenesis of CA-CRC is multifactorial, the formation of tumors in the large bowel is mainly due to environmental factors (such as lifestyle, dietary, and microorganisms) because the heritability of CRC only accounts for 12–35% [4, 5]. Among environmental factors, the role of microorganisms (both specific infectious agents and collective microbial communities in the tumor environment) in CRC has received increasing attention in recent years [6]. Resident microbial communities, including bacteria, fungi, and virus (~ 100 trillion) colonized in the human gastrointestinal tract, called the "gut microbiota" [7]. These microorganisms have been reported to play a crucial role in maintaining mucus barrier function, regulating inflammation and immune responses [6], and thus preventing or promoting intestinal-associated diseases, such as ulcerative colitis (UC) [8] and colitis-associated (CA)-CRC [9]. As an important component of gut microbiota, probiotics, especially *Lactobacillus* and *Bifidobacterium*, are important for attenuating the incidence and mortality of

CA-CRC. For example, the relative abundance of *Lactobacillus* was lower in an azoxymethane (AOM)/dextran sulfate sodium (DSS) induced CA-CRC mouse model as compared with healthy animals [10]. Moreover, treatment with *Lactobacillus casei* BL23 could inhibit the development of CA-CRC caused by AOM/DSS [11]. In addition, supplementation of *Lactobacillus bulgaricus* has been shown to significantly suppress inflammation in the CA-CRC mouse [12]. The anti-CRC effects of probiotics can be summarized as (1) improving host immune defense; (2) inactivating cancerogenic compounds; (3) modulating intestinal microbiota, and (4) regulating the apoptosis and differentiation of tumor cells [13]. However, the use of probiotics as agents to prevent or alleviate CA-CRC is still limited due to the species-specific effects of microorganisms that may further lead to distinct mechanistic actions. Therefore, it is necessary to explore more probiotic strains with CA-CRC ameliorating effects and pay more attention to their functional mechanism.

Lactobacillus coryniformis MXJ32, a heterofermentative facultative anaerobic bacterium, was previously isolated from a traditional fermented vegetable (*Jiangshui Cai*) in Xixiang County, Shaanxi, China [14]. This strain has been shown to possess potential beneficial effects because it not only possesses a certain degree of acid and bile salt tolerance, but also can produce a novel bacteriocin to inhibit the growth of bacterial foodborne pathogens including antibiotic-resistant microorganisms [14]. Moreover, *L. coryniformis* MXJ32 could ameliorate the pathological symptoms of DSS-induced UC in mice [15]. Since the adverse changes in the gut microbiota [16] and long-term colitis [17] may lead to the formation and progression of CA-CRC, it was hypothesized that administration with *L. coryniformis* MXJ32 could reshape a new balance of gut microbiota and inhibit inflammation in AOM/DSS induced CA-CRC mice, thereby inhibiting intestinal tumor formation. Moreover, to our knowledge, no previous study has focused on evaluating the CA-CRC ameliorating effects of *L. coryniformis*. Therefore, the present study aimed to investigate the attenuating effects of *L. coryniformis* MXJ32 on AOM/DSS induced CA-CRC through intestinal barrier integrity, gut microenvironment and inflammatory response. The results of the present study can facilitate the application scope of *L. coryniformis* MXJ32 as a probiotic to prevent or attenuate CA-CRC, and provide the knowledge for further research on the exploration of safe and effective preventive and therapeutic strategies for CA-CRC.

Materials and methods

Preparation of *L. coryniformis* MXJ32

L. coryniformis MXJ32 was previously stored in the de Man, Ragosa, and Sharpe (MRS) broth medium with 20% (v/v) glycerol at − 80 °C. To prepare live bacterial supplement, *L. coryniformis* MXJ32 was grown in MRS medium at 37 °C for 16 h and harvested by centrifugation at 7500×*g* for 5 min at 4 °C. The collected cells were washed twice with cold 0.90% NaCl solution and then resuspended in 0.90% NaCl solution at a concentration of 5×10^9 CFU/mL for oral gavage.

Animals and treatment

Six-week-old male C57BL/6 mice were purchased from Hunan SJA Laboratory Animal Co., Ltd. (Changsha, Hunan, China) and housed in the standard polycarbonate cages (five mice per cage) under a specific pathogen-free controlled environment (temperature 23 ± 2 °C, relative humidity 55 ± 5%, and 12 h light/dark cycle) with ad libitum access to normal chow diet and water. All experimental protocols were approved by the Animal Ethics Committee of Xi'an Jiaotong University (Permission No. SCXK 2018–001) and conducted in compliance with the Guide for the Care and Use of Laboratory Animals: Eighth Edition, ISBN-10: 0-309-15396-4.

After 7 days of acclimatization, forty mice were randomly divided into three groups: Ctrl group (neither AOM/DSS nor *L. coryniformis* MXJ32 treatment, $n = 10$), Model group (only AOM/DSS treatment, $n = 15$), and MXJ32 group (both AOM/DSS and *L. coryniformis* MXJ32 treatment, $n = 15$). The detailed experimental scheme is shown in Fig. 1a. Briefly, the mice in the Model and MXJ32 groups were given a single intraperitoneal (i.p.) injection of AOM (10 mg/kg, Sigma-Aldrich, St. Louis, MO, USA) 7 days before the start of 3 cycles of DSS (MW 36–50 kDa, MP Biomedicals, Aurora, OH, USA) treatment. For each cycle of DSS induction, mice were received water containing 2% DSS (w/v) for 7 consecutive days, followed by 2 weeks of normal drinking water for an adjustable recovery period. The mice in the MXJ32 group were orally administered 200 µL bacterial suspension (~ 1×10^9 CFU/day/mouse) since the beginning of the second cycle of DSS induction and maintained for 14 weeks until sacrifice. The mice in the Ctrl and Model groups were gavaged with the equivalent volume of 0.90% NaCl solution during the same period. Water consumption, body weight, fecal consistency, and blood in the stool of all mice were monitored weekly. At the end of week 18, mice were euthanized with ketamine and xylazine (100 and 10 mg/kg, respectively; i.p. injection, Sigma-Aldrich). Serum samples were obtained by centrifuging blood samples at 3000×*g* at 4 °C for 10 min and then stored at − 80 °C until analysis. The entire colon tissue was harvested, excised, and cleaned with cold phosphate buffer saline (PBS) for macroscopic change assessment. The number and diameter of tumors were measured by an independent observer who was unaware of the treatment. The spleen and thymus were also

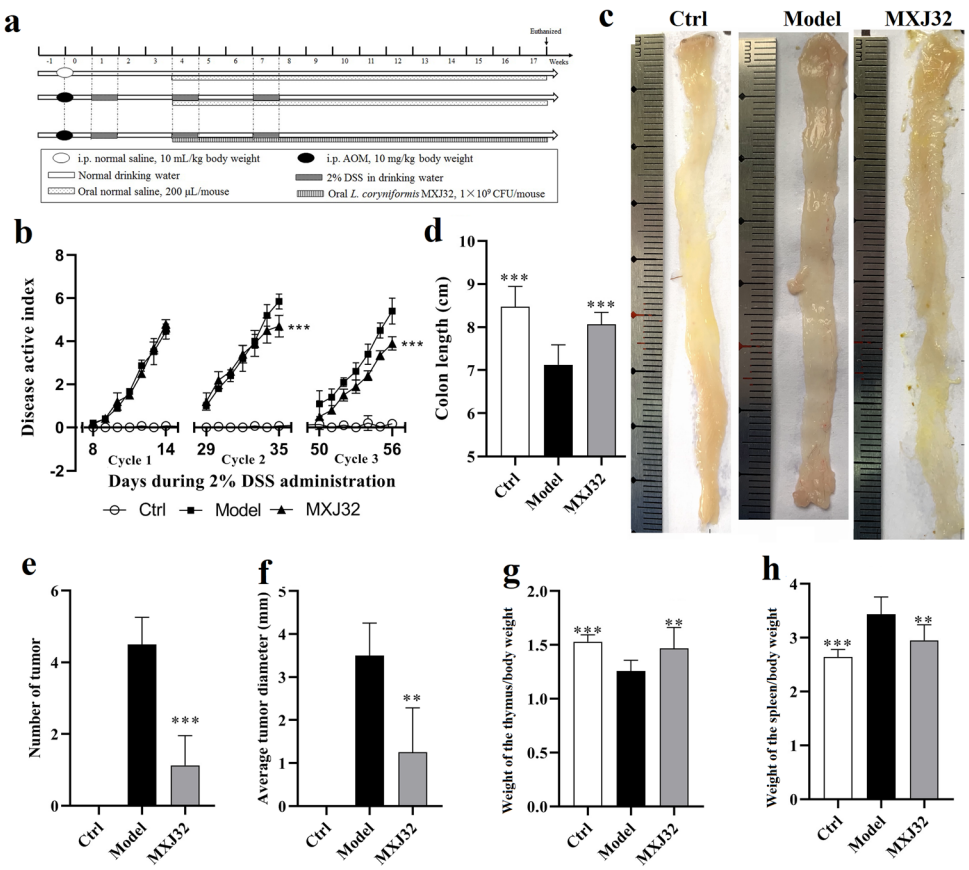

Fig. 1 Effects of *L. coryniformis* MXJ32 on the intestinal tumorigenesis in the AOM/DSS-induced CA-CRC mouse model. **a** the experimental protocol of *L. coryniformis* MXJ32 administration; **b** disease activity index; **c** the representative macroscopic image of mouse colonic tissues; **d** colon length; **e** total tumor number; **f** average tumor diameter (mm); **g** weight of the thymus/body weight; **h** weight of the spleen/body weight. Data are presented as mean ± SD, $n = 10$/group, significant differences were calculated by one-way ANOVA, followed by Tukey's test for multiple comparisons, $^{**}p < 0.01$ and $^{***}p < 0.001$ compared to the Model group

removed to calculate the weight of the organ/body weight [18].

During the DSS induction period, intestinal inflammation was assessed daily by measuring the disease activity index (DAI). It consists of body weight loss ($0 = \leq 1\%$, $1 = 1\% < X \leq 5\%$, $2 = 5\% < X \leq 10\%$, $3 = 10\% < X \leq 15\%$, and $4 = > 15\%$), stool consistency (0 = normal, 1 = soft and sticky, and 4 = diarrhea) and blood in the feces (0 = normal, 1 = occult^{+}, 2 = occult^{++}, 3 = occult^{+++}, and 4 = gross bleeding) [11]. The blood in the feces was tested using the fecal occult blood reagent (Nanjing Jiancheng Technol, Nanjing, Jangshu, China).

Intestinal permeability analysis

To investigate the intestinal permeability of mice, fluorescein isothiocyanate (FITC)-dextran (3000–5000 kDa, Sigma-Aldrich) was given to mice by oral gavage according to the method described by Yang et al. [19] with some minor modifications. Briefly, mice in each group ($n = 3$) were fasted for 6 h and then administered with FITC-dextran (600 mg/kg body weight) for another 4 h of fasting treatment. Mice blood samples were collected by retro-orbital bleeding and centrifuged at 3000 × *g* for 10 min at 4 °C. After diluted (1:1) in PBS (pH 7.4), the fluorescence intensity of mice serum was quantified using a Multi-Mode Microplate Reader (VictorX3, Perkin Elmer, USA) with an excitation wavelength of 485 nm and an emission wavelength of 535 nm. The standard curve was calculated by diluting FITC-dextran in PBS.

Histopathological evaluation

The distal colon tissues (~ 1 cm) were fixed in 4% paraformaldehyde (w/v) at 4 °C overnight, embedded in paraffin, and then sliced into 5 μm for hematoxylin and eosin (H&E), and Alcian blue staining, as well as terminal deoxynucleotidyl transferase dUTP nick end labeling (TUNEL) analysis. The stained areas were viewed and photographed by an Olympus microscope (Olympus Corporation, Tokyo, Japan). The damage of colon tissues was scored as described previously [20], which consists of the severity of inflammation (0–3), the infiltration degree of inflammation (0–3) and the extent of crypt damage (0–4). The number of goblet cells and TUNEL-positive cells was calculated by Image J software (National Institutes of Health, Bethesda, MD, USA).

Biochemical analysis

Lipopolysaccharides (LPS) and colonic inflammatory cytokines, including tumor necrosis factor (TNF-α),

interleukin (IL)-1β, and IL-6 were measured by corresponding ELISA test kits (Jingmei Biotech, Yancheng, Jiangsu, China). For the quantification of colonic inflammatory cytokines, colon tissues were weighed and homogenized with PBS (1:9, w/v), and centrifuged at 5000×*g* for 5 min at 4 °C. The protein concentration in the supernatant was measured by BCA protein assay kit (Zhonghuihecai Biotech, Xi'an, Shaanxi, China).

Quantitative PCR analysis

The total RNA from colon tissues was extracted using AG RNAex Pro Reagent (Accurate Biology, Changsha, Hunan, China). After qualitative and quantitative evaluation by micro-spectrophotometer Nano-200 (Hangzhou Allsheng Instruments, Korea), the FastKing RT Kit (with gDNase, Tiangen Biotech, Beijing, China) was used for reverse transcription immediately. Subsequently, 2 μL diluted cDNA (1:15) was performed quantitative PCR using CFX96 Touch™ Real-Time PCR Detection System (Bio-Rad, Hercules, CA, USA) with SYBR Green BioEasy Master Mix (Bioer Biotech, Hangzhou, Zhejiang, China). The primer sequences of target genes are shown in Table S1. The expression level of target gene was normalized using the mRNA level of housekeeping gene *GAPDH* and the data were analyzed according to the $2^{-\Delta\Delta Ct}$ method.

Short-chain fatty acids (SCFAs) analysis

The concentration of SCFAs was analyzed by gas chromatography (GC) as previously described protocols [21] with some minor modifications. Briefly, ~ 200 mg fecal samples were homogenized with 2 mL distilled water and centrifuged at 10,000×*g* for 10 min at 4 °C. The ratio (weight of fecal sample/volume of distilled water = 1:10) was determined by our preliminary experimental result. The supernatant (0.8 mL) was acidified by adding 160 μL of 50% H_2SO_4 (v/v) for 5 min, and then incubated with 0.8 mL diethyl ether at 4 °C with shaking for 30 min. The organic phase was collected by centrifuging at 10,000×*g* for 10 min and filtered through a 0.22 μm nylon filter for GC analysis. The GC-2014C (Shimadzu Corporation, Kyoto, Japan) equipped with a DB-FFAP column (30 m × 0.25 μm × 0.25 μm, Agilent Technologies, Palo Alto, CA, USA) and a flame ionization detector. Standard SCFAs curves were prepared using acetic acid, propionic acid, isobutyric, butyric acid, isovaleric, and valeric acid (Sigma-Aldrich, St. Louis, MO, USA).

Fecal microbiota analysis

The total bacterial DNA of each fecal sample was extracted using PowerSoil DNA isolation kit (Mo Bio Laboratories, Carlsbad, CA, USA). After qualitative and quantitative analysis by NanoDropOne (Thermo Fisher Scientific, Waltham, MA, USA), the 16S rRNA gene comprising V3–V4 variable regions was amplified by PCR with common primers (Forward primer, 5′-ACTCCTACGGGAGGCAGCA-3′; reverse primer, 5′-GGACTACHVGGGTWTCTAAT-3′). The pooled and purified PCR products were sequenced using Illumina Hiseq 2500 platform at Biomarker Technologies Corporation (Beijing, China). The high-quality reads with ≥ 97% similarity were clustered into the same operational taxonomic unit (OTU) and annotated based on the SILVA database (version 123) using Ribosomal Database Project (RDP) Classifier (version 2.2). The alpha diversity, including Simpson, Shannon, ACE, and Chao indexes, was calculated using Mothur (version 1.30). The Bray–Curtis principal coordinate analysis (PCoA) and unweighted pair group method with arithmetic mean (UPGMA) clustering analysis were performed with the Quantitative Insights Into Microbial Ecology (QIIME) software. The linear discriminant analysis (LDA) coupled with effect size (LEfSe) method was used to analyze the significant changes in the relative abundance of microbial taxa among different groups.

Correlation analysis

The correlation between the genera with significant differences in gut microbiota among three groups and CRC parameters (including DAI and histological scores, colon length, number of tumors, goblet, and TUNEL-positive cells, intestinal permeability, the expression of inflammatory cytokines and chemokines, the level of SCFAs) was analyzed in R language. The correlation between the indicators was quantified by calculating Pearson correlation coefficients and the results were visualized by Corrplot R package.

Statistical analysis

All experimental data were presented as the mean ± standard deviation (SD) of at least three independent experiments. Significant differences were determined by one-way analysis of variance (ANOVA), followed by Tukey's test for multiple comparisons using Graphpad Prism 8 software (GraphPad Software Inc., San Diego, CA, USA). Comparison of significant changes in the relative abundance of microbial taxa between different groups was performed using non-parametric Kruskal–Wallis test. A value of $p < 0.05$ was considered as statistically significant ($^{*}p < 0.05$, $^{**}p < 0.01$ and $^{***}p < 0.001$ compared to the Model group).

Results

L. coryniformis MXJ32 administration ameliorated the development of intestinal tumorigenesis induced by AOM/DSS

CA-CRC is a model of colon carcinogenesis associated with inflammation. To gain insight into the role of *L. coryniformis* MXJ32 in colitis, the DAI score was calculated during 2% DSS administration. Results showed that the DAI score in the MXJ32 group was significantly reduced as compared with the Model group at the end of DSS administration (Fig. 1b). For colon length, treatment with *L. coryniformis* MXJ32 could prevent its shortening caused by DSS (Fig. 1d). In addition, as two important immune organs, the thymus and spleen were also used to reflect the level of inflammation. From Fig. 1g, h, it was shown that the decrease of weight of the thymus/body weight and the increase of weight of the spleen/body weight induced by AOM/DSS were significantly reversed by supplementation of *L. coryniformis* MXJ32. These results suggested that the DSS-induced colon inflammation was successfully established and administration with *L. coryniformis* MXJ32 could alleviate it. For the representative macroscopic image of mouse colonic tissues, there were multiple adenomas in the Model group, while these symptoms were remarkably attenuated in the MXJ32 group (Fig. 1c). Moreover, the total tumor number and average tumor diameter in the MXJ32 group were also significantly lower than those in the Model group (Fig. 1e, f).

Histological examination conducted by H&E staining from the representative distal colon tissues showed that AOM/DSS-treated mice supplementation of *L. coryniformis* MXJ32 had fewer pathological damage symptoms, including the severity and infiltration degree of inflammation and the extent of crypts damage (Fig. 2a, c). A histology of the representative tumor is shown in Fig. S1. Furthermore, Alcian blue staining showed that supplementation of *L. coryniformis* MXJ32 could significantly suppress AOM/DSS-induced mucosal damage and attenuate the loss of goblet cells (Fig. 2b, d). In addition, the number of TUNEL-positive cells in the MXJ32 group was significantly increased as compared with the Model group (Fig. S2a, b), which was also demonstrated by the promoting effect of *L.*

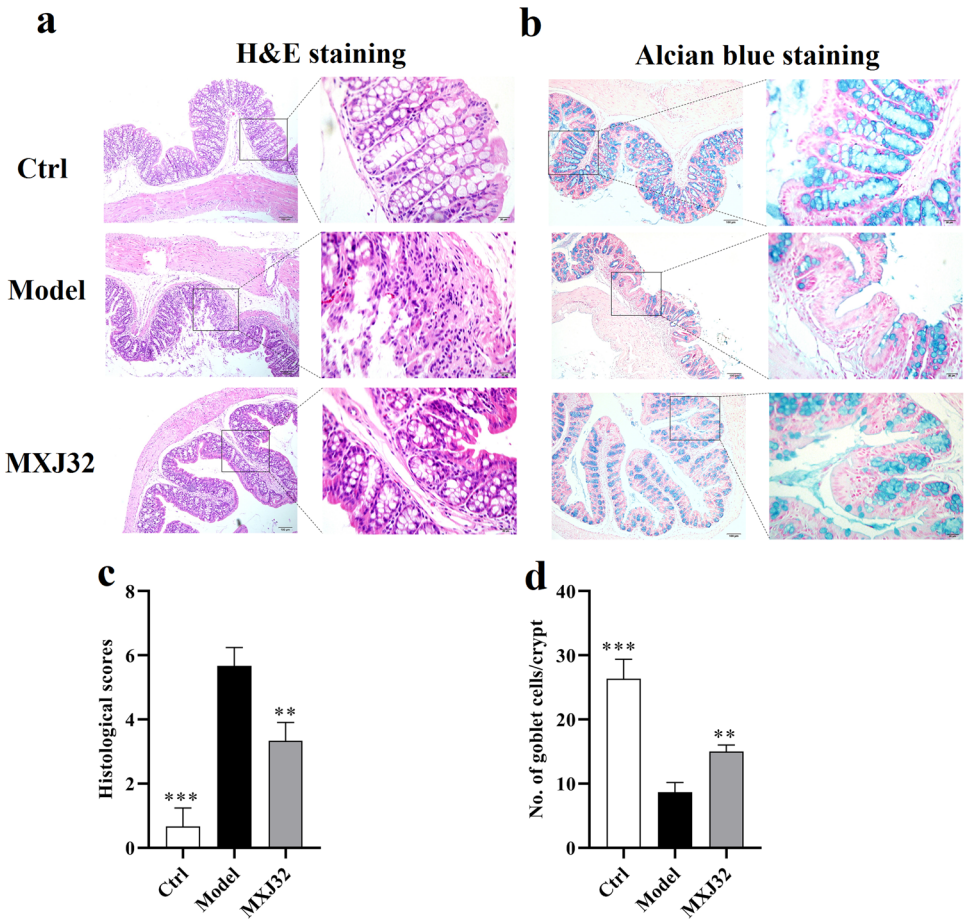

Fig. 2 Effects of *L. coryniformis* MXJ32 on the intestinal histopathological changes in the AOM/DSS-induced CA-CRC mouse model. Representative image of **a** H&E and **b** Alcian blue staining; **c** the histological score, and **d** the number of goblet cells based on H&E- and Alcian blue-stained sections, respectively. Data are presented as mean ± SD, $n = 5$/group, significant differences were calculated by one-way ANOVA, followed by Tukey's test for multiple comparisons, $^{*}p < 0.05$, $^{**}p < 0.01$, and $^{***}p < 0.001$ compared to the Model group

coryniformis MXJ32 administration on the mRNA level of Bax/Bcl-2 (Fig. S2c).

L. coryniformis MXJ32 administration protected the intestinal barrier integrity in the AOM/DSS-induced CA-CRC mice

To evaluate whether *L. coryniformis* MXJ32 could ameliorate the damage of intestinal barrier function, FITC-dextran was used to analyze intestinal permeability. Result showed that AOM/DSS led to an increase in the gut leakage of oral TITC-dextran, while this change was significantly prevented by supplementation of *L. coryniformis* MXJ32 (Fig. 3a). In addition, the expression of some colonic proteins that are related to maintaining intestinal barrier integrity, including occludin, claudin-1, tight junction protein-1 (ZO-1), mucin-2 (MUC2), mucin-3 (MUC3), and trefoil factor-3 (TFF3), was also measured. Although no significant differences were found in the mRNA levels of *MUC2*, *MUC3,* and *TFF3* between the Model and the MXJ32 group, the expression of *Occludin*, *Claudin-1*, and *ZO-1* were significantly downregulated in the AOM/DSS-induced mice, and these alterations were remarkably reversed by *L. coryniformis* MXJ32 administration (Fig. 3b). These results suggested that supplementation of *L. coryniformis* MXJ32 could attenuate the damage of intestinal barrier induced by AOM/DSS.

L. coryniformis MXJ32 administration modulated the inflammatory response in the AOM/DSS-induced CA-CRC mice

Inflammatory cytokines (including TNF-α, TNF-1β, and IL-6) were measured by ELISA kits. Compared with the Ctrl group, the level of these three pro-inflammatory cytokines was significantly increased in the AOM/DSS-treated mice, while treatment with *L. coryniformis* MXJ32 could conspicuously attenuate these changes (Fig. 4a–c). Moreover, the mRNA level of *TNF-α*, *TNF-1β*, *IL-6*, *IL-γ,* and *IL-17a* in the MXJ32 group was also significantly lower than those in the Model group (Fig. 4d).

The abnormal level of CXCR2 ligands, including Cxcl1, Cxcl2, Cxcl3, Cxcl5, and Ccl7, has been found in previous CA-CRC mouse model [22]. Similarly, the results of the present study also showed that AOM/DSS can lead to a significant increase in the mRNA level of *Cxcl1*, *Cxcl2*, *Cxcl3*, *Cxcl5,* and *Ccl7*. On the contrary, these changes were significantly ameliorated after treatment with *L. coryniformis* MXJ32 (Fig. 4e).

As an important activator of Toll-like receptor 4 (TLR4), LPS was an inducement to trigger inflammatory response. From Fig. 4f, the level of serum LPS was significantly increased in the Model group and it could be reversed by *L. coryniformis* MXJ32 supplementation. Moreover, the mRNA level of some genes that related to TLR4/NF-κB pathway (including *TLR4*, *MyD88,* and *NF-κB*) in the model group was higher than that in the MXJ32 group (Fig. 4g–i).

L. coryniformis MXJ32 administration promoted the production of SCFAs in the AOM/DSS-induced CA-CRC mice

It was reported that SCFAs showed multiple beneficial effects against CA-CRC, therefore, the effects of *L. coryniformis* MXJ32 on the level of feces SCFAs were measured. A representative chromatogram of SCFAs in *L. coryniformis* MXJ32 treated mice feces sample is illustrated in Fig. S3.

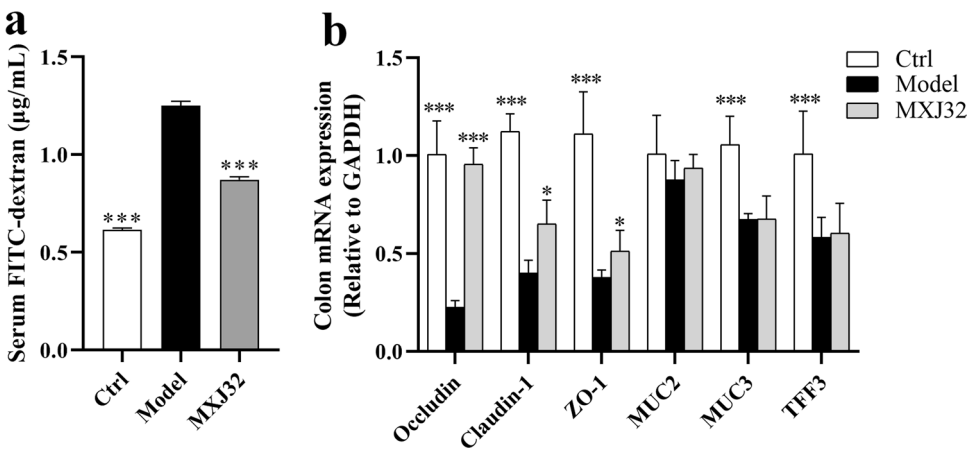

Fig. 3 Effects of *L. coryniformis* MXJ32 on the gut barrier integrity in the AOM/DSS-induced CA-CRC mouse model. **a** The level of serum FITC; **b**, the mRNA expression of *Occludin*, *Claudin-1*, *ZO-1*, *MUC2*, *MUC3*, and *TFF3* in the mouse colon. Data are presented as mean ± SD, n = 5/group, significant differences were calculated by one-way ANOVA, followed by Tukey's test for multiple comparisons, $^{*}p < 0.05$, $^{**}p < 0.01$, and $^{***}p < 0.001$ compared to the Model group

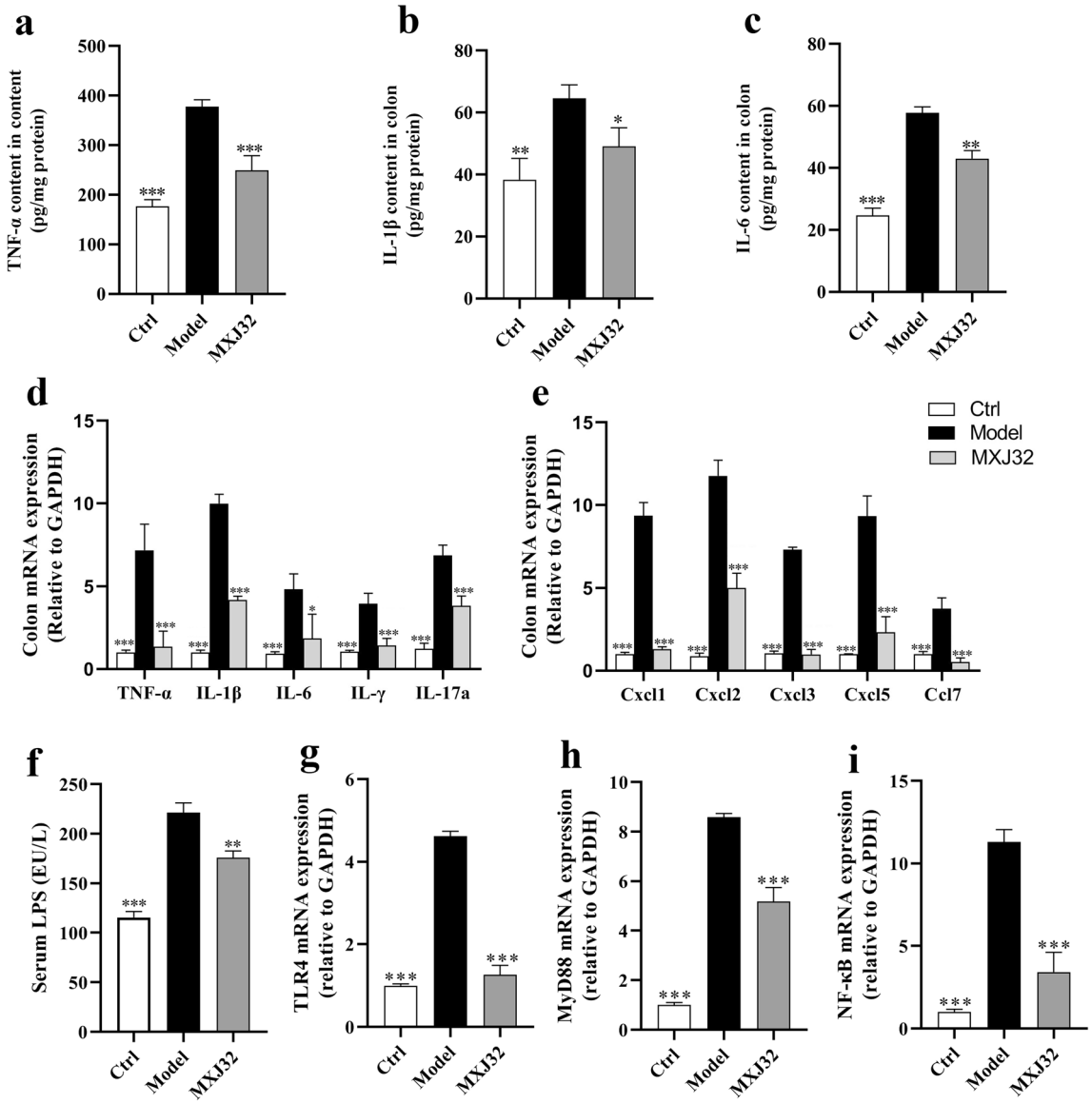

Fig. 4 Effects of *L. coryniformis* MXJ32 on the inflammatory response in the AOM/DSS-induced CA-CRC mouse model. The level of **a** TNF-α, **b** IL-1β, and **c** IL-6 in mouse colon; **d** the mRNA expression of *TNF-α*, *IL-1β*, *IL-6*, *IL-γ*, and *IL-17a* in mouse colon; **e** the mRNA expression of chemokines, including *Cxcl1*, *Cxcl2*, *Cxcl3*, *Cxcl5*, and *Ccl7*; **f** the level of serum LPS; the mRNA expression of **g** *TLR 4*, **h** *MyD88*, and **i** *NF-κB*. Data are presented as mean ± SD, $n = 5$/group, significant differences were calculated by one-way ANOVA, followed by Tukey's test for multiple comparisons, $^{*}p < 0.05$, $^{**}p < 0.01$ and $^{***}p < 0.001$ compared to the Model group

From Fig. 5a, b, the major three SCFAs produced by gut microbiota are acetic, propionic, and butyric acid. The total SCFAs concentration was significantly decreased in the Model group, whereas it was reversed by treatment with *L. coryniformis* MXJ32 (Fig. 5b). Specifically, compared with the Ctrl group, the levels of propionic, butyric acid, isobutyric, and isovaleric were significantly decreased in the Model group. Except for isovaleric, the other SCFAs were significantly increased after treatment with *L. coryniformis* MXJ32 (Fig. 5a). These results suggested that the anti-carcinogenic effect of *L. coryniformis* MXJ32 in the CA-CRC mouse model might be partly due to it increases the level of SCFAs.

L. coryniformis MXJ32 administration altered the composition of gut microbiota in the AOM/DSS-induced CA-CRC mice

Overall, 978,034 available reads (Ctrl, 347,786; AOM, 304,442 MXJ32, 325,806) from 15 samples were obtained for the downstream analysis, and 4253 OTUs were identified with a 97% similarity cutoff (data not shown). Rarefaction

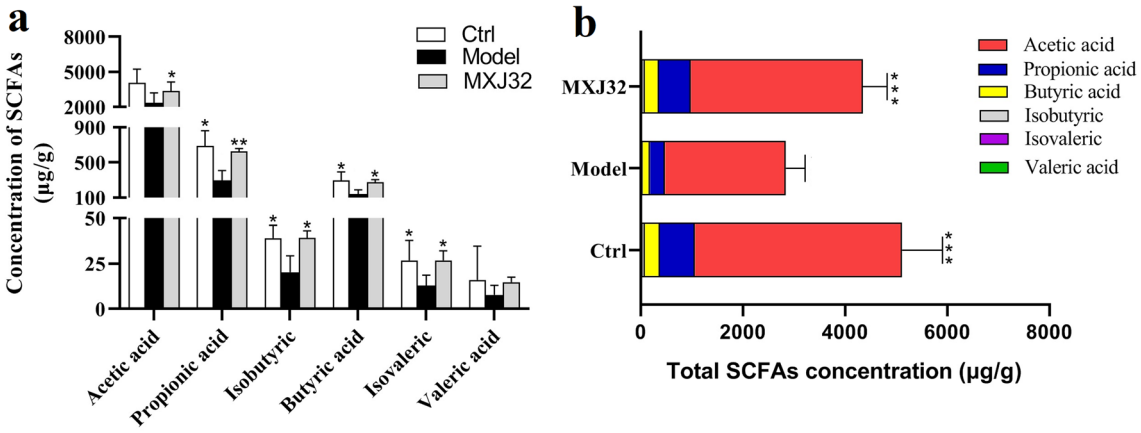

Fig. 5 Effects of *L. coryniformis* MXJ32 on the SCFAs concentration in the mice feces. **a** The levels of acetic acid, propionic acid, isobutyric, butyric acid, isovaleric and valeric acid; **b**, the levels of total SCFAs. Data are presented as mean ± SD, $n = 5$/group, significant differences were calculated by one-way ANOVA, followed by Tukey's test for multiple comparisons, $^{*}p < 0.05$ and $^{***}p < 0.001$ compared to the Model group

and Shannon curves are shown in Fig. S4, suggesting that the majority of the microbiota diversity has been captured in all samples and the OTUs in the Model group are higher than those in the Ctrl and MXJ32 groups. There was no statistical difference in the microbiota community richness (ACE and Chao indices), but the microbiota diversity (Shannon and Simpson indices) in the Model group was significantly different from that in the Ctrl and MXJ32 groups (Fig. 6a). For beta diversity, the results of PCoA based on Bray–Curtis analysis are shown in Fig. 6b, suggesting that the samples in the Model group were separated from the Ctrl group, while the MXJ32 group tended to cluster toward the Ctrl group, which could also be reflected by the UPGMA analysis (Fig. 6c). These results demonstrated that treatment with *L. coryniformis* MXJ32 could attenuate gut microbiota dysbiosis induced by AOM/DSS. Briefly, compared with the Ctrl group, a higher abundance of phylum Bacteroidetes, Proteobacteria, Patescibacteria, and Epsilonbacteraeota, and a lower abundance of Actinobacteria were observed in the Model group, while supplementation of *L. coryniformis* MXJ32 weakened these alterations (Fig. 6d). The genus-level analysis showed that there were 15 genera with significant differences among the three groups (Table S2). For example, compared with the Ctrl group, the relative abundance of some beneficial bacteria (such as *Lactobacillus*, *Bifidobacterium*, *Akkermansia*, and *Faecalibaculum*) and harmful bacteria (such as *Desulfovibrio* and *Helicobacter*) in the Model group were significantly decreased and increased, respectively. However, these changes were reversed by treatment with *L. coryniformis* MXJ32 (Fig. 6e).

In the correlation analysis, except for *Bacteroides* and *Lachnospiraceae_NK4A136_group*, the other 13 genera were almost negatively or positively correlated with CA-CRC parameters (Fig. 7). Briefly, the genera *Lactobacillus*, *Bifidobacterium*, *Akkermansia*, and *Faecalibaculum* were positively correlated with colon length, goblet cells and SCFAs, and negatively correlated with DAI and histological scores, intestinal permeability, LPS, CXCR2 levels and inflammatory cytokines, suggesting that these genera may have a role in alleviating CA-CRC. Oppositely, the genera *Parasutterella*, *uncultured_bacterium_f_Ruminococcaceae*, *Desulfovibrio*, *Coriobacteriaceae_UCG-002*, *Helicobacter*, *Candidatus_Saccharimonas*, *uncultured_bacterium_f_Lachnospiraceae* and *Ruminiclostridium_9* were positively correlated with parameters that could promote CA-CRC and negatively correlated with parameters that could prevent CA-CRC (Fig. 7).

To further investigate the specific significantly different phylotypes in response to *L. coryniformis* MXJ32 administration, LEfSe analysis was performed on all effective sequences. Compared with Ctrl group, there were eight (including genera *uncultured_bacterium_f_Muribaculaceae*, *Family_XIII_UCG_001*, *Eisenbergiella*, *Family_XIII_AD3011_group*, *Lachnospiraceae_UCG_006*, *uncultured_bacterium_f_Lachnospiraceae*, *Roseburia*, *Ruminiclostridium_9* and *Ruminiclostridium*) and five (including genera *Alistipes*, *Ruminococcaceae_UCG_013*, *Bacteroides*, *Eubacterium_xylanophilum*, *Parabacteroides,* and *Ruminococcus_1*) specific genera in the Model and MXJ32 group, respectively (Fig. 8a–d). Moreover, compared with Model group, there were five (including *Odoribacter*, *Eubacterium_fissicatena_group*, *Akkermansia*, *Bifidobacterium* and *Lactobacillus*), and one (*Ruminococcaceae_UCG_013*) specific genera in the Ctrl and MXJ32 group, respectively (Fig. 8a, b, e, f). In addition, compared with the MXJ32 group, there were two (including *uncultured_bacterium_f_Ruminococcaceae* and *Clostridium_sensu_stricto_1*) and six (including

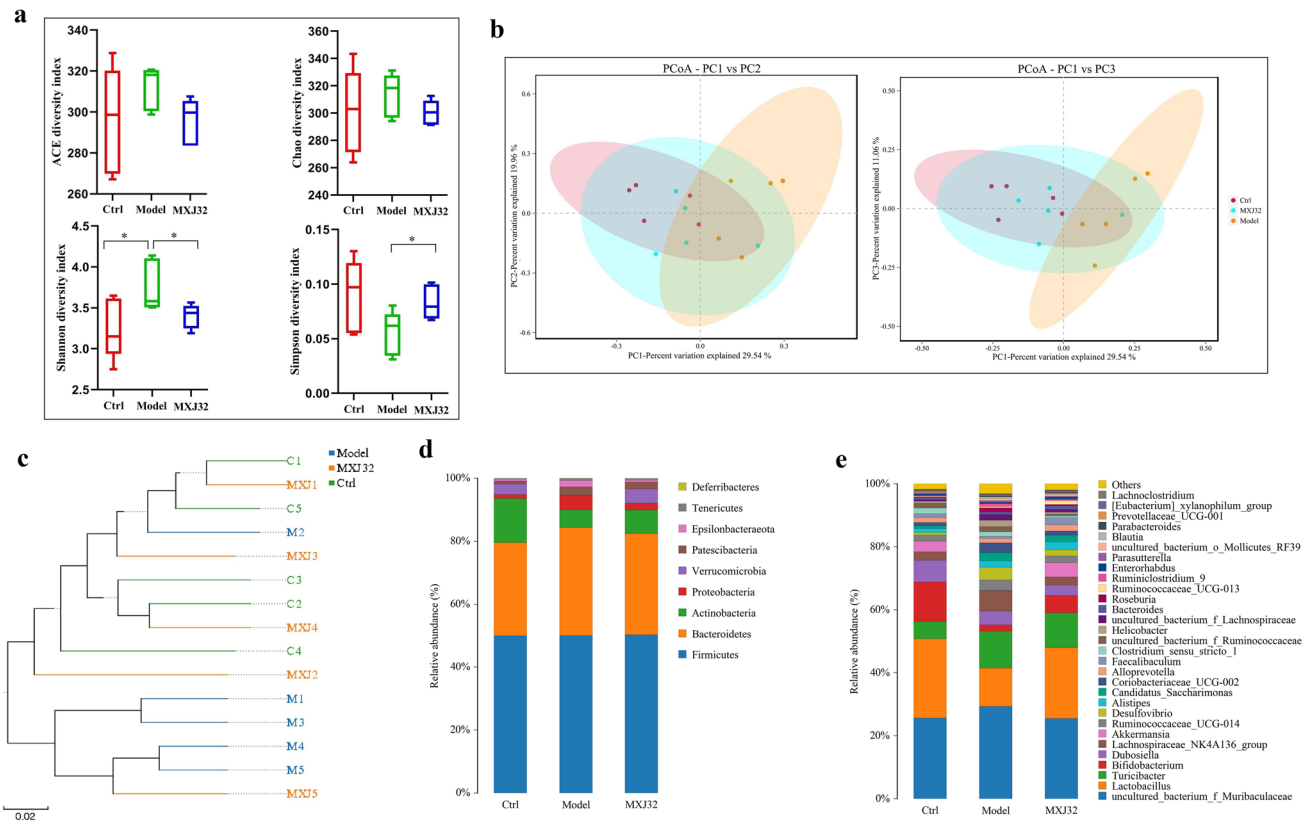

Fig. 6 Effects of *L. coryniformis* MXJ32 on the composition of the gut microbiota in the AOM/DSS-induced CA-CRC mouse model. **a** Alpha diversity including ACE, Chao, Shannon and Simpson analysis; **b** principal coordinate analysis (PCoA) based on Bray–Curtis analysis; **c** hierarchical clustering tree on OTU level determined by multivariate analysis of variance from PCoA matrix scores; microbiota composition at **d** phylum and **e** genus level. $n = 5$/group, significant differences were calculated by one-way ANOVA, followed by Tukey's test for multiple comparisons, $^{*}p < 0.05$

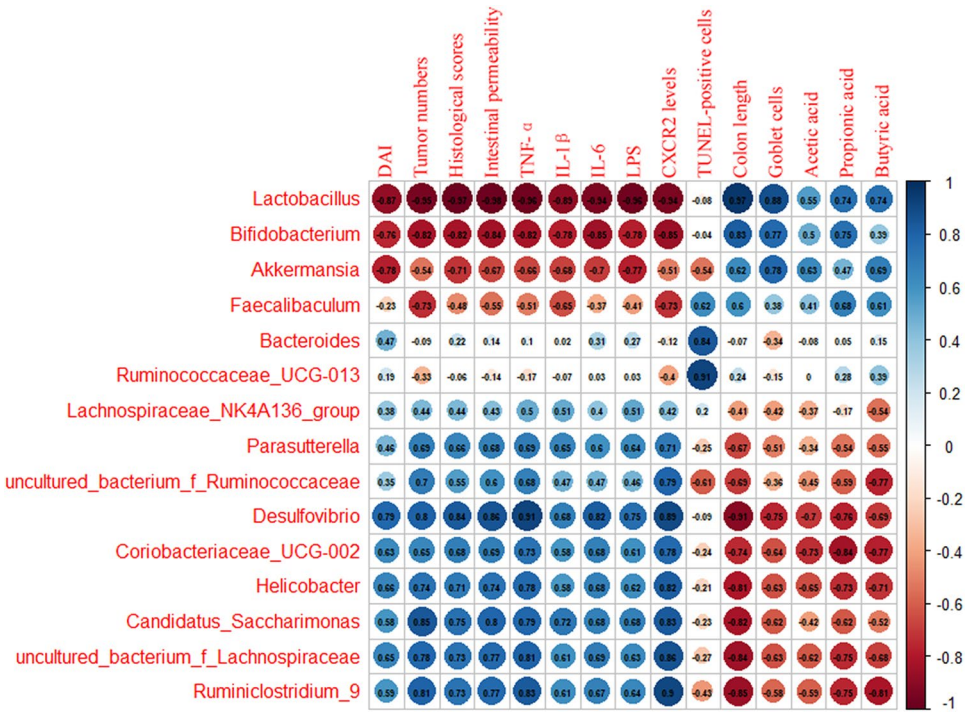

Fig. 7 Correlation analysis between 15 genera and CRC parameters. DAI is presented by the data at the end of the third DSS induction; intestinal permeability is presented by the level of serum TITC-dextran; CXCR2 levels are the total level of Cxcl1, Cxcl2, Cxcl3, Cxcl5, and Ccl7

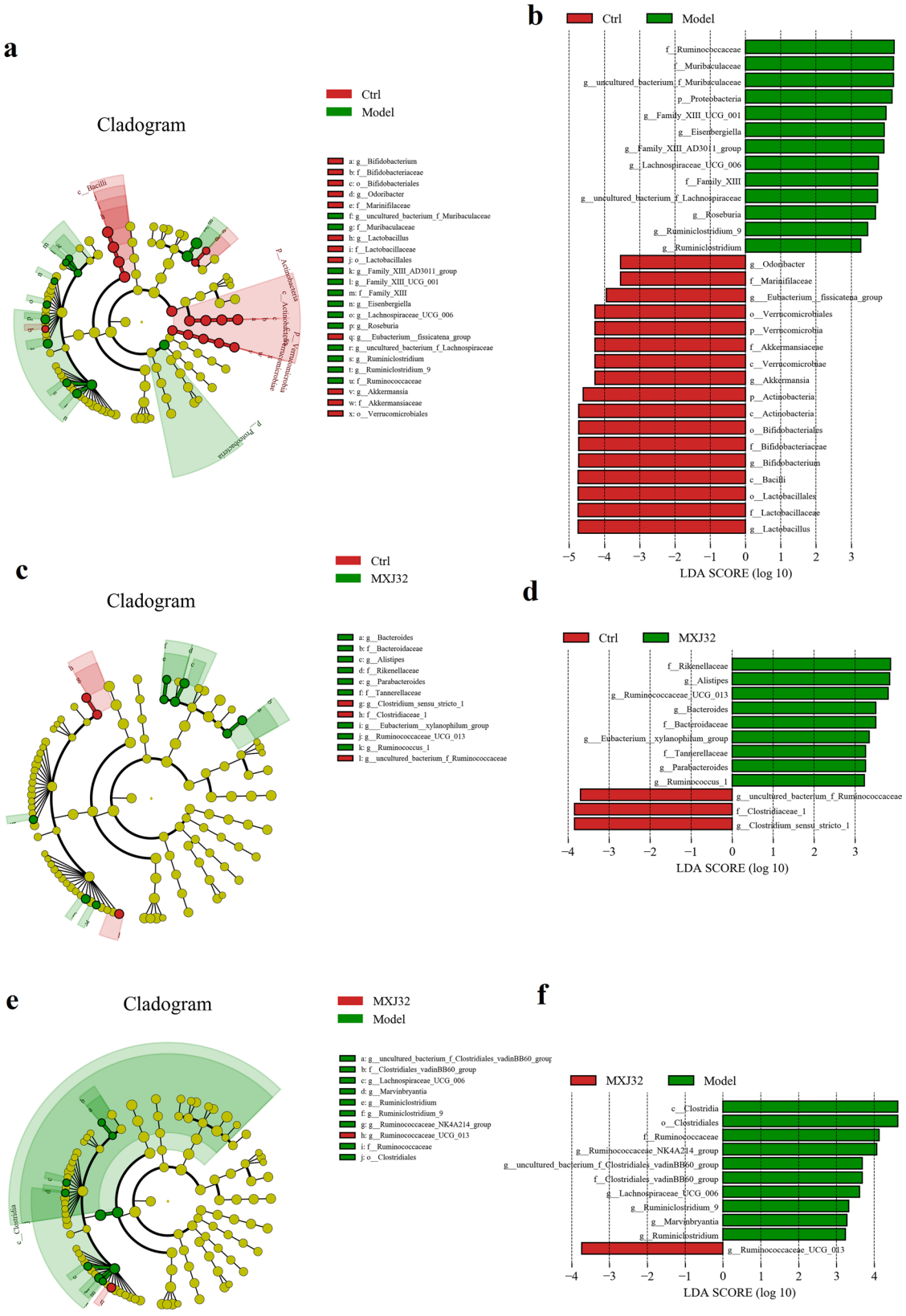

Fig. 8 Screening of differentially abundant microbial taxa using linear discriminant analysis (LDA) coupled with effect size (LEfSe) analysis. LEfSe cladogram of the discriminative microbial taxa (**a** Ctrl vs Model; **c** Ctrl vs MXJ32; **e** Model vs MXJ32), the size of the circle shows the relative abundance of the taxa and yellow dots indicate no statistical significance; LEfSe score plot of the discriminative microbial taxa (**b** Ctrl vs Model; **d** Ctrl vs MXJ32; **f** Model vs MXJ32). Only the taxa with LDA score > 3.0 are shown

Ruminococcaceae, *Ruminococcaceae_NK4A214_group*, *uncultured_bacterium_f_Clostridiales_vadinBB60_group*, *Lachnospiraceae_UCG_006*, *Ruminiclostridium_9*, *Marvinbryantia*, *Ruminiclostridium*) specific genera in the Ctrl and Model group, respectively (Fig. 8c–f). Taken together, these results indicated that AOM/DSS induces a major alteration in gut microbiota composition, whereas *L. coryniformis* MXJ32 supplementation could be at least partly reverse this dysbiosis.

Discussion

Most findings suggested that the intestinal microenvironment of patients with CA-CRC was significantly different from that of healthy individuals [16, 23]. Therefore, in recent years, regulation of intestinal microbiota was considered to be a promising method to prevent CA-CRC. Previously, *L. coryniformis* MXJ32 has been shown to have the ability to inhibit bacterial foodborne pathogens, including antibiotic-resistant microorganisms by producing a novel bacteriocin [14]. Moreover, this probiotic could ameliorate the pathological symptoms of DSS-induced UC in mice [15]. However, whether treatment with *L. coryniformis* MXJ32 could inhibit intestinal tumor formation via reshaping intestinal microbiota and suppressing inflammation has not been studied. Therefore, this study aimed to investigate the anti-carcinogenic effect of *L. coryniformis* MXJ32 in the AOM/DSS-induced CA-CRC mouse model. Compared with the Model group, the DAI score, total tumor numbers and average tumor diameter in the MXJ32 group were significantly reduced (Fig. 1), suggesting the recovery of damaged colon cells effect of *L. coryniformis* MXJ32. These were also evidenced by the histology results, including preventing inflammatory infiltration, crypt damage and goblet cell loss (Fig. 2).

CA-CRC has been proven to be strongly associated with chronic inflammation, and the risk of CA-CRC in patients with inflammatory bowel disease (IBD) showed 2–8 times higher than that of healthy individuals [24]. Therefore, the incidence of CA-CRC could be effectively prevented by inhibiting the inflammatory response [25]. In this study, the increase of some pro-inflammatory cytokines (such as TNF-α, IL-1β, IL-6, IL-γ, and IL-17a) induced by AOM/DSS was significantly inhibited via supplementation of *L. coryniformis* MXJ32 (Fig. 4a–d). In addition, compared with the Model group, the mRNA expression of CXCR2 ligands, including *Cxcl1*, *Cxcl2*, *Cxcl3*, *Cxcl5*, and *Ccl7*, was also remarkably decreased after treatment with *L. coryniformis* MXJ32 (Fig. 4e), which was similar to the finding of Song et al. [22] who reported that these CXCR2 chemokines were significantly down-regulated in the probiotic cocktail Bifico treated CA-CRC mice. The abnormal expression of these chemokines was responsible for recruiting inflammatory cells into the inflammatory bowel mucosa and promoting tumor initiation, progression, angiogenesis, and metastasis [26]. Therefore, the anti-tumorigenesis effects of *L. coryniformis* MXJ32 may be partly due to its anti-inflammatory properties in the CA-CRC mice. However, further study is needed to investigate the effect of *L. coryniformis* MXJ32 on the specific immune response, especially the effect on the differentiation of immune cell. In addition, there was an important point to be mentioned that the result of TUNEL-staining in the present study showed that the number of TUNEL-positive cells in the probiotic-treated group was higher than that in the Model group. In the DSS-induced UC mouse model, the number of these positive cells in the colitis Model group was higher than that in the colitis ameliorating group [27]. Inversely, these number in the CRC mouse polyp was lower than that in the CRC alleviating mouse [28]. Although the distal colon tissue (a site of high incidence of tumor and polyp in the CA-CRC mouse model) was selected to conducted TUNEL-staining in the present study, it was still not completely suggested that supplementation of *L. coryniformis* MXJ32 could promote the apoptosis of tumor cells because the cell apoptosis in the Model and MXJ32 group consists of both the normal cell apoptosis of normal mucosa and the apoptosis of tumor damaged mucosal cells. Therefore, it is necessary to conduct TUNEL-staining on both with and without tumors/polyps colon tissue to investigate whether treatment with *L. coryniformis* MXJ32 could promote the apoptosis of tumor cells.

Patients with colitis-associated disease are generally accompanied with the damage of intestinal barrier function [29, 30]. To adapt to the rapidly changing conditions of intestinal microenvironment, maintaining the integrity of intestinal barrier was essential to ensure tissue sterility and selective permeability of nutrients [31]. Microbial pathogens and intestinal inflammation could damage the intestinal barrier function and lead to increased intestinal permeability, translocation of various microbial substances and immune activation [32]. Meanwhile, the damage of gut barrier could result in increased translocation of bacteria and lead to chronic inflammation, which could further induce carcinogenic processes via IL-6 and STAT3 signaling [33]. Supplementation of *L. coryniformis* MXJ32 in the AOM/DSS-induced CA-CRC mice showed that it could ameliorate the damage of intestinal barrier via preventing the decrease of tight junctions-associated genes expression (such as Occludin, Claudin-1, and ZO-1) (Fig. 3), which in turn suggested that treatment with *L. coryniformis* MXJ32 could prevent microorganisms from entering the internal circulatory system through the epithelial barrier and further attenuate the inflammatory response that caused by gut microbial pathogens.

The composition of intestinal microbiota was highly related to the occurrence and formation of CA-CRC [34]. Some literature reported that supplementation of probiotics could prevent colon tumorigenesis by modulating gut microbiota [35, 36]. The results of this study showed that *L. coryniformis* MXJ32 administration could partly restore the change of intestinal microbiota in the AOM/DSS-induced CA-CRC mice and impel them more similar to that of healthy mice (Fig. 6). The cross-talk between gut microbiota and intestinal epithelial may play an important role in regulating intestinal immune homeostasis [37]. The genus-level analysis in the present study suggested that the relative level of some proinflammatory bacteria, such as *Desulfovibrio* and *Helicobacter*, was significantly increased in the Model group (Fig. 6e), which was accompanied with higher intestinal inflammation. Oppositely, treatment with *L. coryniformis* MXJ32 could not only reverse these microbiota alterations but also alleviate inflammatory responses. In the LEfSe analysis, consistent with some previous reports, the genera of *Akkermansia*, *Bifidobacterium* and *Lactobacillus* were the significant phylotypes in the healthy mouse as compared with the CA-CRC Model mouse [38, 39]. However, compared with the Ctrl group, some genera, such as *Eisenbergiella*, *Family_XIII_AD3011_group*, and *Ruminiclostridium_9* were found the significant phylotypes in the Model group, which suggested that these genera could be further identified as potential biomarkers for CA-CRC prognostication. Compared with the Model group, only genus *Ruminococcaceae_UCG_013* was the significant phylotype in the *L. coryniformis* MXJ32 treated group, suggesting this genus may have potential CA-CRC ameliorating effect. This is similar to the finding of Wang et al. [39] who reported that treatment with *B. bifidum* CGMCC 15068 in the CA-CRC mouse could significantly increase the abundance of *Ruminococcaceae_UCG_013*.

The activation of TLR4/NF-κB in intestinal epithelial cells was considered to be an important pathway to promote colitis-associated tumorigenesis [17]. Microbial pathogens and LPS, two major activators of TLR4, were found at higher levels in the AOM/DSS-induced CA-CRC mice (Figs. 4f, g, 6e), which was similar to the results reported by Fukata et al. [40] As the final effector molecule of TLR4 signaling pathway, NF-κB plays a crucial role in causing inflammatory response [17, 41]. Our results showed that administration with *L. coryniformis* MXJ32 could significantly decrease the level of LPS (Fig. 4f) and the abundance of some harmful bacteria (such as *Desulfovibrio* and *Helicobacter*), and thus attenuate the overactivation of TLR4/MyD88/NF-κB pathway, which further inhibit the secretion of pro-inflammatory cytokines (such as TNF-α, IL-1β, IL-6) and chemokines.

Compared with the Model group, the relative abundance of *Lactobacillus*, *Bifidobacterium*, *Akkermansia*, and *Faecalibaculum* was higher in the *L. coryniformis* MXJ32 treated group (Fig. 6e). These bacteria belong to SCFAs-producing bacteria [38, 42] and correspond to higher levels of SCFAs in the MXJ32 group (Fig. 5). SCFAs have been shown to play an important role in preventing intestinal diseases, such as IBD and CRC [43]. Previous literature reported that SCFAs could inhibit the growth of some pathogens in the host intestinal microenvironment [44]. Therefore, besides the effect of bacteriocin produced by *L. coryniformis* MXJ32, it could be speculated that the decrease of some pro-inflammation bacteria, such as *Desulfovibrio* and *Helicobacter*, in the MXJ32 group may be also the antibacterial effect of SCFAs. In addition, SCFAs, especially butyric acid, have been proved to have potential benefits for CA-CRC patients as they could promote and maintain colonic epithelial health [32], moderate cell growth and differentiation [45], inhibit histone deacetylases in colonocytes and immune cells [46] and exert anti-inflammatory effect [47]. Therefore, the increases of SCFAs caused by *L. coryniformis* MXJ32 administration may be also partly responsible for its anti-carcinogenic effect in the CA-CRC mouse model.

Together, these results demonstrated that treatment with *L. coryniformis* MXJ32 could prevent the disruption of intestinal microbiota, including the increase of beneficial bacteria (such as SCFAs-producing bacteria, *Lactobacillus*, *Bifidobacterium*, *Akkermansia*, and *Faecalibaculum*) and the decrease of harmful bacteria (such as pro-inflammatory bacteria, *Desulfovibrio*, and *Helicobacter*). Moreover, the damage of intestinal barrier integrity was alleviated under the inhibition of microbial pathogens and intestinal inflammation, which could further prevent the translocation of microbial pathogens and harmful bacterial substances (such as LPS) from the gut to the systemic circulation, and in turn suppress the overactivation of TLR4/NF-κB pathway and inhibit the secretion of pro-inflammatory cytokines (such as TNF-α, IL-1β, IL-6) and chemokines. Therefore, treatment with *L. coryniformis* MXJ32 could ameliorate AOM/DSS-induced CA-CRC via reshaping intestinal microenvironment, alleviating inflammation, and intestinal barrier damage. These results could promote *L. coryniformis* MXJ32 as a probiotic to alleviate CA-CRC, and provide the knowledge for further exploration of probiotics as a safe and effective preventive strategy for CA-CRC. Although it was confirmed that *L. coryniformis* MXJ32 could attenuate CA-CRC, the specific pathway of this ameliorating effect is not clear. The molecular mechanism of *L. coryniformis* MXJ32 on gut microbiota and gut inflammatory immune would be further studied in the future.

Supplementary Information The online version contains supplementary material available at https://doi.org/10.1007/s00394-021-02627-8.

Acknowledgements The author thanks the financial support of Post-doctoral Start-up funding (2018) of Northwest A&F University (Z109021804) and National Natural Science Foundation of China (Grant no. 31972043 and 32001652).

Author contributions TW, BL, XW, and XL designed the study and wrote the manuscript; TW and LZ performed the experiments; PW and YL analyzed the data; TW, GW, and YS interpreted the results of experiments; YY and YZ prepared figures. All authors read and approved the final manuscript.

Data availability The datasets generated and/or analyzed during the current study are available from the corresponding author on reasonable request.

Declarations

Conflict of interest The authors have no conflicts of interest.

Ethics declarations All animal experiments were conducted according to the Guide for the Care and Use of Laboratory Animals: Eighth Edition, ISBN-10: 0-309-15396-4, and were approved by the Animal Ethics Committee of Xi'an Jiaotong University (Permission No. SCXK 2018-001).

References

1. Bray F, Ferlay J, Soerjomataram I, Siegel RL, Torre LA, Jemal A (2018) Global cancer statistics 2018: GLOBOCAN estimates of incidence and mortality worldwide for 36 cancers in 185 countries. CA Cancer J Clin 68(6):394–424. https://doi.org/10.3322/caac.21492
2. Yin L, Meng Z, Zhang YX, Hu KK, Chen WY, Han KB, Wu BY, You R, Li CH, Jin Y, Guan YQ (2018) *Bacillus* spore-based oral carriers loading curcumin for the therapy of colon cancer. J Control Release 271:31–44. https://doi.org/10.1016/j.jconrel.2017.12.013
3. Yue YC, Ye K, Lu J, Wang XY, Zhang SW, Liu L, Yang BY, Nassar K, Xu XX, Pang XY, Lv JP (2020) Probiotic strain *Lactobacillus plantarum* YYC-3 prevents colon cancer in mice by regulating the tumour microenvironment. Biomed Pharmacother 127:1–8. https://doi.org/10.1016/j.biopha.2020.110159
4. O'Brien JM (2000) Environmental and heritable factors in the causation of cancer: analyses of cohorts of twins from Sweden, Denmark, and Finland, by P. Lichtenstein, N.V. Holm, P.K. Verkasalo, A. Iliadou, J. Kaprio, M. Koskenvuo, E. Pukkala, A. Skytthe, and K. Hemminki. N Engl J Med 343:78-84, 2000. Surv Ophthalmol 45(2):167–168. https://doi.org/10.1016/s0039-6257(00)00165-x
5. Czene K, Lichtenstein P, Hemminki K (2002) Environmental and heritable causes of cancer among 9.6 million individuals in the Swedish family-cancer database. Int J Cancer 99(2):260–266. https://doi.org/10.1002/ijc.10332
6. Wong SH, Yu J (2019) Gut microbiota in colorectal cancer: mechanisms of action and clinical applications. Nat Rev Gastroenterol Hepatol 16(11):690–704. https://doi.org/10.1038/s41575-019-0209-8
7. Donaldson GP, Lee SM, Mazmanian SK (2016) Gut biogeography of the bacterial microbiota. Nat Rev Microbiol 14(1):20–32. https://doi.org/10.1038/nrmicro3552
8. Tian Y, Zhou Y, Huang SS, Li J, Zhao K, Li XH, Wen XC, Li XA (2019) Fecal microbiota transplantation for ulcerative colitis: a prospective clinical study. BMC Gastroenterol 19:12. https://doi.org/10.1186/s12876-019-1010-4
9. Uronis JM, Muhlbauer M, Herfarth HH, Rubinas TC, Jones GS, Jobin C (2009) Modulation of the intestinal microbiota alters colitis-associated colorectal cancer susceptibility. PLoS ONE 4(6):e6026. https://doi.org/10.1371/journal.pone.0006026
10. Li YH, Wang S, Sun Y, Xu WQ, Zheng HN, Wang Y, Tang Y, Gao XW, Song C, Long Y, Liu JY, Liu L, Mei QB (2020) Apple polysaccharide protects ICR mice against colitis associated colorectal cancer through the regulation of microbial dysbiosis. Carbohydr Polym 230:10. https://doi.org/10.1016/j.carbpol.2019.115726
11. Jacouton E, Chain F, Sokol H, Langella P, Bermudez-Humaran LG (2017) Probiotic strain *Lactobacillus casei* BL23 prevents colitis-associated colorectal cancer. Front Immunol 8:10. https://doi.org/10.3389/fimmu.2017.01553
12. Silveira DSC, Veronez LC, Lopes LC, Anatriello E, Brunaldi MO, Pereira-da-Silva G (2020) *Lactobacillus bulgaricus* inhibits colitis-associated cancer via a negative regulation of intestinal inflammation in azoxymethane/dextran sodium sulfate model. World J Gastroenterol 26(43):6782–6794. https://doi.org/10.3748/wjg.v26.i43.6782
13. Eslami M, Yousefi B, Kokhaei P, Hemati M, Nejad ZR, Arabkari V, Namdar A (2019) Importance of probiotics in the prevention and treatment of colorectal cancer. J Cell Physiol 234(10):17127–17143. https://doi.org/10.1002/jcp.28473
14. Lu X, Yi LH, Dang J, Dang Y, Liu BF (2014) Purification of novel bacteriocin produced by *Lactobacillus coryniformis* MXJ32 for inhibiting bacterial foodborne pathogens including antibiotic-resistant microorganisms. Food Control 46:264–271. https://doi.org/10.1016/j.foodcont.2014.05.028
15. Wang T, Sun H, Chen J, Luo L, Gu Y, Wang X, Shan Y, Yi Y, Liu B, Zhou Y, Lu X (2021) Anti-adhesion effects of *Lactobacillus* strains on Caco-2 cells against *Escherichia Coli* and their application in ameliorating the symptoms of dextran sulfate sodium-induced colitis in mice. Probiotics Antimicrob Proteins. https://doi.org/10.1007/s12602-021-09774-8
16. Chen WG, Liu FL, Ling ZX, Tong XJ, Xiang C (2012) Human intestinal lumen and mucosa-associated microbiota in patients with colorectal cancer. PLoS ONE 7(6):9. https://doi.org/10.1371/journal.pone.0039743
17. Yao DB, Dong M, Dai CL, Wu SD (2019) Inflammation and inflammatory cytokine contribute to the initiation and development of ulcerative colitis and its associated cancer. Inflamm Bowel Dis 25(10):1595–1602. https://doi.org/10.1093/ibd/izz149
18. Sun J, Chen H, Kan J, Gou YR, Liu J, Zhang X, Wu XN, Tang SX, Sun R, Qian CL, Zhang NF, Niu FX, Jin CH (2020) Anti-inflammatory properties and gut microbiota modulation of an alkali-soluble polysaccharide from purple sweet potato in DSS-induced colitis mice. Int J Biol Macromol 153:708–722. https://doi.org/10.1016/j.ijbiomac.2020.03.053
19. Yang HX, Wang WC, Romano KA, Gu M, Sanidad KZ, Kim D, Yang J, Schmidt B, Panigrahy D, Pei RS, Martin DA, Ozay EI, Wang YX, Song MY, Bolling BW, Xiao H, Minter LM, Yang GY, Liu ZH, Rey FE, Zhang GD (2018) A common antimicrobial additive increases colonic inflammation and colitis-associated colon tumorigenesis in mice. Sci Transl Med 10(443):10. https://doi.org/10.1126/scitranslmed.aan4116
20. Xie F, Zhang H, Zheng C, Shen XF (2020) Costunolide improved dextran sulfate sodium-induced acute ulcerative colitis in mice through NF-kappa B, STAT1/3, and Akt signaling pathways. Int Immunopharmacol 84:10. https://doi.org/10.1016/j.intimp.2020.106567
21. Wang T, Yan H, Lu YY, Li X, Wang X, Shan YY, Yi YL, Liu BF, Zhou Y, Lu X (2020) Anti-obesity effect of *Lactobacillus rhamnosus* LS-8 and *Lactobacillus crustorum* MN047 on high-fat and high-fructose diet mice base on inflammatory response

alleviation and gut microbiota regulation. Eur J Nutr 59(6):2709–2728. https://doi.org/10.1007/s00394-019-02117-y
22. Song H, Wang WY, Shen B, Jia H, Hou ZY, Chen P, Sun YW (2018) Pretreatment with probiotic Bifico ameliorates colitis-associated cancer in mice: transcriptome and gut flora profiling. Cancer Sci 109(3):666–677. https://doi.org/10.1111/cas.13497
23. Cammarota R, Bertolini V, Pennesi G, Bucci EO, Gottardi O, Garlanda C, Laghi L, Barberis MC, Sessa F, Noonan DM, Albini A (2010) The tumor microenvironment of colorectal cancer: Stromal TLR-4 expression as a potential prognostic marker. J Transl Med 8:16. https://doi.org/10.1186/1479-5876-8-112
24. van Staa TP, Card T, Logan RF, Leufkens HG (2005) 5-Aminosalicylate use and colorectal cancer risk in inflammatory bowel disease: a large epidemiological study. Gut 54(11):1573–1578. https://doi.org/10.1136/gut.2005.070896
25. Flores BM, O'Connor A, Moss AC (2017) Impact of mucosal inflammation on risk of colorectal neoplasia in patients with ulcerative colitis: a systematic review and meta-analysis. Gastrointest Endosc 86(6):1006-1011.e1008. https://doi.org/10.1016/j.gie.2017.07.028
26. Wang DZ, DuBois RN, Richmond A (2009) The role of chemokines in intestinal inflammation and cancer. Curr Opin Pharmacol 9(6):688–696. https://doi.org/10.1016/j.coph.2009.08.003
27. Wang K, Jin X, Li Q, Sawaya ACHF, Le Leu RK, Conlon MA, Wu L, Hu F (2018) Propolis from different geographic origins decreases intestinal inflammation and *Bacteroides* spp. populations in a model of DSS-induced colitis. Mol Nutr Food Res 62(17):1800080. https://doi.org/10.1002/mnfr.201800080
28. Khazaie K, Zadeh M, Khan MW, Bere P, Gounari F, Dennis K, Blatner NR, Owen JL, Klaenhammer TR, Mohamadzadeh M (2012) Abating colon cancer polyposis by *Lactobacillus acidophilus* deficient in lipoteichoic acid. Proc Natl Acad Sci USA 109(26):10462–10469. https://doi.org/10.1073/pnas.1207230109
29. Soroosh A, Rankin CR, Polytarchou C, Lokhandwala ZA, Patel A, Chang L, Pothoulakis C, Iliopoulos D, Padua DM (2019) miR-24 Is elevated in ulcerative colitis patients and regulates intestinal epithelial barrier function. Am J Pathol 189(9):1763–1774. https://doi.org/10.1016/j.ajpath.2019.05.018
30. Katinios G, Casado-Bedmar M, Walter SA, Vicario M, Gonzalez-Castro AM, Bednarska O, Soderholm JD, Hjortswang H, Keita AV (2020) Increased colonic epithelial permeability and mucosal eosinophilia in ulcerative colitis in remission compared with irritable bowel syndrome and health. Inflamm Bowel Dis 26(7):974–984. https://doi.org/10.1093/ibd/izz328
31. Robrahn L, Jiao L, Cramer T (2020) Barrier integrity and chronic inflammation mediated by HIF-1 impact on intestinal tumorigenesis. Cancer Lett 490:186–192. https://doi.org/10.1016/j.canlet.2020.07.002
32. Sun J, Kato I (2016) Gut microbiota, inflammation and colorectal cancer. Genes Dis 3(2):130–143. https://doi.org/10.1016/j.gendis.2016.03.004
33. Zeisel MB, Dhawan P, Baumert TF (2019) Tight junction proteins in gastrointestinal and liver disease. Gut 68(3):547–561. https://doi.org/10.1136/gutjnl-2018-316906
34. Kang MS, Martin A (2017) Microbiome and colorectal cancer: unraveling host-microbiota interactions in colitis-associated colorectal cancer development. Semin Immunol 32(C):3–13. https://doi.org/10.1016/j.smim.2017.04.003
35. Gao ZG, Guo BM, Gao RY, Zhu QC, Wu W, Qin HL (2015) Probiotics modify human intestinal mucosa-associated microbiota in patients with colorectal cancer. Mol Med Report 12(4):6119–6127. https://doi.org/10.3892/mmr.2015.4124
36. Wierzbicka A, Mankowska-Wierzbicka D, Mardas M, Stelmach-Mardas M (2021) Role of probiotics in modulating human gut microbiota populations and activities in patients with colorectal cancer-a systematic review of clinical trials. Nutrients 13(4):13. https://doi.org/10.3390/nu13041160
37. Peck BCE, Mah AT, Pitman WA, Ding SL, Lund PK, Sethupathy P (2017) Functional transcriptomics in diverse intestinal epithelial cell types reveals robust microRNA sensitivity in intestinal stem cells to microbial status. J Biol Chem 292(7):2586–2600. https://doi.org/10.1074/jbc.M116.770099
38. Oh NS, Lee JY, Kim YT, Kim SH, Lee JH (2020) Cancer-protective effect of a synbiotic combination between *Lactobacillus gasseri* 505 and a *Cudrania tricuspidata* leaf extract on colitis-associated colorectal cancer. Gut Microbes 12(1):20. https://doi.org/10.1080/19490976.2020.1785803
39. Wang Q, Wang KC, Wu WR, Lv LX, Bian XY, Yang LY, Wang QQ, Li YT, Ye JH, Fang DQ, Wu JJ, Jiang XW, Xie JJ, Lu YM, Li LJ (2020) Administration of *Bifidobacterium bifidum* CGMCC 15068 modulates gut microbiota and metabolome in azoxymethane (AOM)/dextran sulphate sodium (DSS)-induced colitis-associated colon cancer (CAC) in mice. Appl Microbiol Biotechnol 104(13):5915–5928. https://doi.org/10.1007/s00253-020-10621-z
40. Fukata M, Chen A, Vamadevan AS, Cohen J, Breglio K, Krishnareddy S, Hsu D, Xu R, Harpaz N, Dannenberg AJ, Subbaramaiah K, Cooper HS, Itzkowitz SH, Abreu MT (2007) Toll-like receptor-4 promotes the development of colitis-associated colorectal tumors. Gastroenterology 133(6):1869–1881. https://doi.org/10.1053/j.gastro.2007.09.008
41. De Simone V, Franze E, Ronchetti G, Colantoni A, Fantini MC, Di Fusco D, Sica GS, Sileri P, MacDonald TT, Pallone F, Monteleone G, Stolfi C (2015) Th17-type cytokines, IL-6 and TNF-alpha synergistically activate STAT3 and NF-kB to promote colorectal cancer cell growth. Oncogene 34(27):3493–3503. https://doi.org/10.1038/onc.2014.286
42. Zagato E, Pozzi C, Bertocchi A, Schioppa T, Saccheri F, Guglietta S, Fosso B, Melocchi L, Nizzoli G, Troisi J, Marzano M, Oresta B, Spadoni I, Atarashi K, Carloni S, Arioli S, Fornasa G, Asnicar F, Segata N, Guglielmetti S, Honda K, Pesole G, Vermi W, Penna G, Rescigno M (2020) Endogenous murine microbiota member *Faecalibaculum rodentium* and its human homologue protect from intestinal tumour growth. Nat Microbiol 5(3):511–524. https://doi.org/10.1038/s41564-019-0649-5
43. Gomes SD, Oliveira CS, Azevedo-Silva J, Casanova MR, Barreto J, Pereira H, Chaves SR, Rodrigues LR, Casal M, Corte-Real M, Baltazar F, Preto A (2020) The role of diet related short-chain fatty acids in colorectal cancer metabolism and survival: prevention and therapeutic implications. Curr Med Chem 27(24):4087–4108. https://doi.org/10.2174/0929867325666180530102050
44. Yao Y, Cai X, Fei W, Ye Y, Zhao M, Zheng C (2020) The role of short-chain fatty acids in immunity, inflammation and metabolism. Crit Rev Food Sci Nutr. https://doi.org/10.1080/10408398.2020.1854675
45. Li M, van Esch B, Wagenaar GTM, Garssen J, Folkerts G, Henricks PAJ (2018) Pro- and anti-inflammatory effects of short chain fatty acids on immune and endothelial cells. Eur J Pharmacol 831:52–59. https://doi.org/10.1016/j.ejphar.2018.05.003
46. Chang PV, Hao LM, Offermanns S, Medzhitov R (2014) The microbial metabolite butyrate regulates intestinal macrophage function via histone deacetylase inhibition. Proc Natl Acad Sci USA 111(6):2247–2252. https://doi.org/10.1073/pnas.1322269111
47. Singh N, Gurav A, Sivaprakasam S, Brady E, Padia R, Shi HD, Thangaraju M, Prasad PD, Manicassamy S, Munn DH, Lee JR, Offermanns S, Ganapathy V (2014) Activation of Gpr109a, receptor for niacin and the commensal metabolite butyrate, suppresses colonic inflammation and carcinogenesis. Immunity 40(1):128–139. https://doi.org/10.1016/j.immuni.2013.12.007